Contents lists available at ScienceDirect

Estuarine, Coastal and Shelf Science

Annual biogeochemical cycling in intertidal sediments of a restored estuary reveals dependence of N, P, C and Si cycles to temperature and water column properties

Dunia Rios-Yunes [*], Justin C. Tiano [1], Dick van Oevelen, Jeroen van Dalen, Karline Soetaert

Royal Netherlands Institute for Sea Research, Estuarine and Coastal Systems Department, Yerseke, 4401NT, the Netherlands

ABSTRACT

Estuarine intertidal sediments are important centres for organic matter remineralization and nutrients recycling. Nevertheless, there is limited understanding regarding how these processes occur along the salinity gradient and their seasonality. Here, we report on the seasonal biogeochemical cycles from three types of intertidal sedimentary habitats (freshwater, brackish and marine) located in the Western Scheldt estuary (The Netherlands and Belgium). A full year of solute fluxes, porewater nutrient and sediment pigment concentrations at a monthly resolution revealed clear differences in the biogeochemistry of the three sites, indicating that environmental conditions determined the local nutrient dynamics. Temperature controlled sediment oxygen consumption rates and nutrient fluxes, but also affected pore water nutrient concentrations up to 14 cm deep. Fresh and brackish sediments had a net influx of dissolved inorganic nitrogen (DIN) (-1.62 mmol m^{-2} d^{-1} and -2.84 mmol m^{-2} d^{-1}, respectively), while only the freshwater sediments showed a net influx of phosphate (-0.07 mmol m^{-2} d^{-1}). We estimated that intertidal sediments remineralized a total of 10,000 t C y^{-1}, with 97% of mineralization occurring in the brackish and marine parts. Overall, sediments removed 11% (1500 t N y^{-1}) and 15% (~200 t P y^{-1}) of the total nitrogen and phosphorus entering the estuary from riverine input. Moreover, observations revealed the historical improvement of water quality resulting from water treatment policies. This spatiotemporal study of OM remineralization and early diagenesis in estuarine systems highlights the importance of intertidal sediments for estuarine systems. Our observations can be used in models to predict estuarine biogeochemistry or assess climate change scenarios.

1. Introduction

Estuaries are centres of transformation, export, and retention of nutrients from terrestrial sources into coastal waters (Arndt et al., 2009; Statham, 2012). They exhibit high heterogeneity of biological (e.g. organism activity and species succession), physical (e.g. salinity, morphology, hydrology, light, tidal regime) and biogeochemical properties (e.g. nutrient concentrations, cycling and fluxes) (Arndt et al., 2009; Magalhães et al., 2002; Middelburg et al., 2005; Statham, 2012). Nutrients entering estuaries have different origins: terrestrial sources such as sewage and fertilizers in the form of ammonium nitrate (NH_4NO_3) and calcium phosphate ($Ca_3(PO_4)_2$) (Billen et al., 2005; Gilbert et al., 2007; Soetaert et al., 2006), inputs from other water bodies

such as rivers and seas (Gilbert et al., 2007), or inputs from sediment-water exchange (Herbert, 1999). The biogeochemical cycling of nutrients and carbon is ultimately driven by the production and degradation of organic matter (OM) from autochthonous (local microphytobenthos and phytoplankton blooms) or allochthonous (terrestrial) origin (Arndt et al., 2013).

OM and nutrient concentrations typically decrease along the salinity gradient from upstream to downstream areas which resembles a filtering effect (Sharp et al., 1984). The filtering effect traps nutrients in the estuary before reaching the sea; its efficiency depends on OM sources and nutrient cycling processes occurring in the water column along the estuarine salinity gradient (Soetaert et al., 2006; Statham, 2012), but also on the exchanges between sediment and water column (Magalhães

---

* Corresponding author.
E-mail addresses: dunia.rios.yunes@nioz.nl (D. Rios-Yunes), justin.tiano@wur.nl (J.C. Tiano), Dick.van.Oevelen@nioz.nl (D. van Oevelen), Jeroen.van.Dalen@nioz.nl (J. van Dalen), Karline.Soetaert@nioz.nl (K. Soetaert).
[1] Present address: Wageningen Marine Research, Wageningen University and Research, PO box 68, 1970 AB, IJmuiden, the Netherlands.

et al., 2002). Examples of such processes include the dilution of riverine water with seawater, *in situ* biogeochemical transformations (Soetaert et al., 2006), uptake by both marine (Arndt et al., 2009; Pastuszak et al., 2008), and terrestrial (siliceous plants in salt marshes) primary producers (Struyf et al., 2005b), and in some cases, wastewater treatment (Brion et al., 2008).

The shallow depth of estuaries together with their high productivity suggest that a great portion of the OM remineralization occurs in the sediment (Jørgensen and Sørensen, 1985). Failing to account for estuarine benthic respiration could overlook around 26% of the global respiration (Middelburg et al., 2005). Furthermore, estuaries provide essential habitats for aquatic and terrestrial organisms and are important centres for nutrient cycling (Lessin et al., 2018) and removal (Magalhães et al., 2002). Research on sediment biogeochemical processes, which fundamentally differ from those occurring in the water column (Cox et al., 2009; Statham, 2012), is important to complement our understanding of estuarine biogeochemistry.

OM is incorporated into the sediment by deposition, benthic organisms, and tidal action where it is remineralized by heterotrophs that sequentially use different terminal electron acceptors (O_2, NO_2^-, NO_3^-, Mn^{4+}, Fe^{3+}, SO_4^{2-}, CO_2) to obtain energy (Arndt et al., 2013). Several biogeochemical processes are constrained to occur near the oxic-anoxic interface, notably, nitrification and denitrification, the sorption and desorption of phosphorus (PO_4^{3-}) onto sediment particles, and the dissolution of biogenic silica (BSi) (Struyf et al., 2005b). Benthic autotrophic OM production as well as heterotrophic activity associated to OM remineralization are affected by seasonal changes. Seasonality - a driver for environmental variability - induces natural fluctuations in temperature and light irradiance that affect the estuarine biological community, nutrient transformation, and exchange (i.e. flux) rates between the sediment and the water column (Arndt et al., 2009; Fang et al., 2019; Jørgensen and Sørensen, 1985; Mestdagh et al., 2020; Soetaert et al., 2006).

Studying the finer-scale spatiotemporal variability of biogeochemical processes is necessary for a better understanding of estuarine bentho-pelagic processes and to assess their response to climate change (Lessin et al., 2018). Some studies have addressed the seasonality of OM remineralization in estuarine mudflats (Bally et al., 2004; Cook et al., 2004; Feuillet-Girard et al., 1997; Khalil et al., 2018; Magalhães et al., 2002; Mestdagh et al., 2020; Mortimer et al., 1999; Van Colen et al., 2012). However, these studies are limited in spatiotemporal resolution (e.g. sampling carried out only once per season or at one station) along the estuarine salinity gradient.

Our study was conducted in the Western Scheldt estuary (WS) between Belgium and The Netherlands. The watershed of the WS and its main tributaries, the Scheldt, Dender, and Rupel rivers, comprises an area of 22,116 km^2 that is subject to large human influence (e.g. urbanization, farming, and industry) (Gilbert et al., 2007; Maris and Meire, 2017; Middelburg et al., 1996; Soetaert and Herman, 1995a). From the 1960's, the implementation of water quality control policies, and the opening of the Brussels-North wastewater treatment plant (WWTP) have improved water quality, eliminated hypoxia, and reduced the concentration of dissolved inorganic phosphorus (DIP) and nitrogen (DIN) entering the Western Scheldt estuary (Brion et al., 2015; Cox et al., 2009; Hofmann et al., 2008; Vanderborght et al., 2007). The WS is therefore a good model for estuarine studies because its water column biogeochemistry has been extensively monitored in its transformation from hypereutrophication with water column hypoxia supporting denitrification to a eutrophic state with year-round oxic conditions (Arndt et al., 2009; Cox et al., 2009; Middelburg et al., 1996; Soetaert et al., 2006; Soetaert and Herman, 1995b). Nevertheless, the role of intertidal sediments in nutrient dynamics in the WS has not been sufficiently addressed. This study analysed monthly samples from three areas of the WS to i) quantify benthic OM remineralization and biogeochemical cycling, ii) assess whether there have been water quality improvements in the past two decades, and iii) calculate the contribution of intertidal sediments to OM mineralization and nutrient retention.

2. Methods

2.1. Study area

The Scheldt River originates in France, flows through a brackish water zone in Belgium, and meets marine water in the WS before discharging into the North Sea (Soetaert et al., 1994b). The WS has a typical funnel-shape, narrow in the upstream, freshwater part (average width <100 m), and then rather abruptly increasing in width past the Belgian-Dutch border until reaching a mean width of 6 km at the mouth (Fig. 1). Its average depth increases from around 3 m near Ghent to 15 m near the mouth at Vlissingen. The funnel shape morphology gives rise to a longitudinal salinity gradient, with low salinities predominating in the narrow section, and a rather steep salinity gradient in the brackish region where the Scheldt becomes wider. The salinity gradient in the brackish region is also influenced by temporal changes in riverine discharge (Baeyens et al., 1997; Soetaert et al., 2006; Struyf et al., 2004). For example, a lower riverine discharge in summer causes a salinity increase in the mesohaline area, because there is less dilution and seawater can reach deeper into the estuary. The discharge of tributaries (Schelde, Dender, and Rupel rivers) into the WS is driven by precipitation and is higher during the winter than in the summer with an average yearly discharge of 120 m^3 s^{-1} (Deltares, 2013; Wang et al., 2019). Sampling was conducted in three intertidal mudflats, close to the main channel, with contrasting salinity and 70% dry time (Fig. 1). The freshwater and brackish sites were adjacent to a reed (*Phragmites australis*) salt marsh.

2.2. Sampling method

Sediment core samples from the intertidal sites were taken monthly from March 2019 to February 2020 during low tide. Core samples were taken for incubations (30 cm long, 15 cm inner diameter (∅); filled to half), porewater (30 cm, 10 cm ∅), and granulometry (30 cm, 3.5 cm ∅). Pigments samples (1 cm^3) were sampled by means of a cut-off syringe (1 cm ∅) in triplicate from the upper 1 cm of the sediment. At each site, 10 L of water was taken, as close as possible to the sampling location. After collection, the cores were transported to The Royal Netherlands Institute for Sea Research, Yerseke (NIOZ- EDS Yerseke). The incubation cores were kept in a thermostatic bath inside a dark ambient temperature-controlled climate room (representing the ambient water
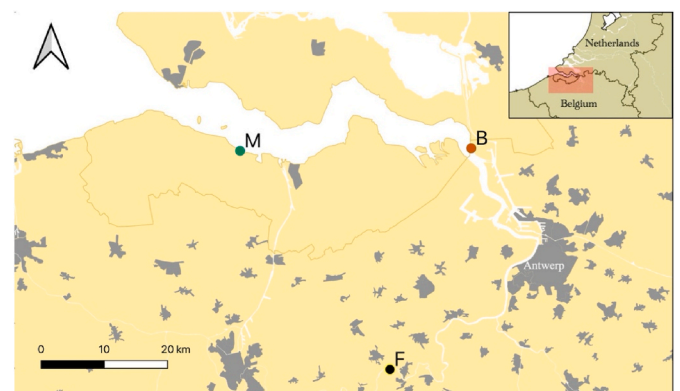

Fig. 1. Map of the intertidal sampling locations. The freshwater (F) site, at Appels, Belgium (51.04832°N, 4.06934°E) is located in the Scheldt River. The brackish (B) location, at Groot Buitenschoor, Netherlands (51.36337°N, 4.24456 °E), and the marine (M) site, in the Paulina Polder, Netherlands (51.35337°N, 3.72054°E) are in the Western Scheldt. Land use in this area is dominated by farmland apart from cities shown in grey. Maps created with QGIS.

temperatures) until the next day to acclimatize. The porewater was immediately extracted upon arrival to the institute and the pigment samples were frozen at -80 °C. The granulometry cores were stored in a 4 °C refrigerator until they were processed on the following day.

Additional water column temperature data for the freshwater (station: Dendermonde SF/Dender) and brackish sites (station: Lillo Meetpaal-Onder SF/Zeeschelde) were obtained from the Flemish Environment Agency, Belgium (Flanders Environment Agency, n.d.), and for the marine site (station: Overloop van Hansweert) from the Dutch Directorate General for Public Works and Water Management (Rijkswaterstaat, n.d.). Water column nutrients from the Ruppel river tributary (Station: 210000) and the Schelde + Dender rivers (Station: 164000) for the sampling period were downloaded from the Geoloket water website (Flanders Environment Agency, n.d.). Discharge values from the Scheldt (station: Dendermonde afw Dender calc/Zeeschelde) and Rupel (station: Wintam Monding calc/Rupel) rivers were obtained from the Flemish Government (Flemish Government, n.d.). Bathymetry data for the year 2021 was provided by Rijkswatersaat (Rijkswaterstaat, n.d.).

2.3. Experimental methods and calculations

The porewater was sampled inside an anoxic glove bag using rhizons (CSS 5 cm, Rhizosphere) at 0 (near the sediment-water interface), 1, 2, 3, 5, 10, and 14 cm depth. Of the extracted porewater, an aliquot of 500 µL was sampled for ammonium (NH_4^+), nitrite (NO_2^-), nitrate (NO_3^-), and Dissolved Si (DSi); and one of 100 µL acidified with 10 µL of 1 M sulfuric acid (Merck, No. 100731) for PO_4^{3-} analysis. Photosynthetic marker pigments were analysed following the method described by Zapata et al. (2000). Pigment samples were freeze dried and analysed with HPLC (LC-04, Shimadzu Co., Kyoto, Japan) with a Waters C8 column (150 × 4.6 mm,3.5 µm particle size, 0.01 µm pore size, nr. WAT200630, Waters Corporation, Milford, MA, USA) connected to a guard cartridge (Symmetry C8 Sentry Guard Cartridge, 100 Å, 5 µm, 3.9 mm × 20 mm, nr. WAT054250, Waters Corporation, Milford, MA, USA) for separation. The pigments were extracted from 1 g of sediment using 90% acetone (Nanograde, nr.1.00658.2500, Promochem) + APO (β-Apo-8′-carotenal) (10 mL). Following extraction, each sample was homogenised and centrifuged, and 800 µL of the supernatant was injected into the HPLC column.

Sediment incubations were performed in dark conditions, to prevent photosynthesis, at ambient temperature. The cores were filled with pre-bubbled water and hermetically sealed with a lid fitted with a magnetic rotor. Oxygen (O_2) concentration in the overlying water was continuously measured with an oxygen optode (Firesting, Pyroscience). The O_2 measurements were stopped when the concentration reached 70% saturation or after ~7 h, after which lids were opened and the overlying water was bubbled. Filtered (Chromdis 0.45 µm, 25 mm, No. 250425) water samples (5 ml) were taken for nutrient (NH_4^+, NO_2^-, NO_3^-, DSi and PO_4^{3-}) analysis at the start of the incubation, the end of the respiration measurement, and after 23, 31 and 48 h. The nutrient samples from the incubations and the porewater samples were refrigerated after collection and analysed with a Segmented Flow Analyzer (QuAAtro39 Auto-Analyzer with XY-2 Sampler Autosampler, SEAL Analytical). Fluxes of O_2 and inorganic nutrients (NH_4^+, NO_2^-, NO_3^-, DSi and PO_4^{3-}) were estimated by fitting a linear regression calculating the change in concentration as a function of time. The fitted slope was multiplied by the height of the overlying water column to obtain the flux. To determine the granulometry, slices of 1 cm thickness were taken at 0, 2, and 4 cm, and from 5 to 10 and 10–14 cm depth. These slices were freeze dried, and analysed by laser diffraction (MALVERN Mastersizer 2000; No. 34403/139, model APA, 2000 with Hydro G 2000 introduction unit). Sediment porosity was calculated from water content and solid-phase measurements accounting for porewater salinity. Organic carbon (OrgC) and N content were determined using an Interscience Flash 2000 organic element analyzer.

The temperature coefficient, Q_{10} value, was calculated based on the respiration rates with the following equation.

$$R_2 = R_1 Q_{10}^{\frac{T_2 - T_1}{10}}$$

where R_1 is the rate of reaction at a first temperature (T_1) and R_2 the rate of reaction at a second temperature (T_2). Graphs and data analysis were created using the computing program R (R Core Team, 2020). The program QGIS was used for geospatial analysis (QGIS Development Team, 2021). Intertidal areas were defined to be between -2 and 2 m NAP (Kuijper and Lescinski, 2013).

3. Results

3.1. Abiotic conditions of the water column and the sediment

Salinity was stable throughout the year at the different locations (Fig. 2 A), apart from a slight increase from May to December at the brackish location. The water temperature fluctuated seasonally at all stations (Fig. 2 B), and for most of the year, was slightly higher at the freshwater and brackish sites compared to the marine site. The water temperature was ≥ 20 °C from July to September at all sites.

Dissolved nutrients varied seasonally (Fig. 3). The concentration of NH_4^+ in the freshwater site (Fig. 3 A) was highest in winter (March 2019 and December 2019 to February 2020) (mean $\pm$ standard deviation; 22.5 ± 1.2 mmol m^{-3}) and lowest from April to November 2019 (4.8 ± 2.4 mmol m^{-3}). Similar dynamics were observed in the brackish site although the seasonality was less pronounced; here the concentration of NH_4^+ fluctuated around 5.4 ± 7.0 mmol m^{-3}. In contrast, NH_4^+ values in the marine site peaked during the summer-autumn reaching a maximum of 18.6 ± 2.4 mmol m^{-3} in October. NO_2^- showed the lowest concentrations during the summer in all sites (Fig. 3 B), except for one high value in August in the brackish site. Largest fluctuations of NO_2^- were observed in the freshwater site, whereas the seasonality was least pronounced in the marine site. The concentration of NO_3^- changed seasonally (Fig. 3 C), with lowest values in the summer months, and decreasing seawards. The freshwater site had the greatest variation in DSi ranging from a high of 235.7 mmol m^{-3} in the colder months while remaining below 50 mmol m^{-3} from May to October (Fig. 3 D). A similar seasonality was observed at the brackish site, where the DSi concentration ranged from 38.0 to 161.7 mmol m^{-3}. In contrast, seasonal fluctuations of DSi were minimal at the marine site and ranged between 13.7 mmol m^{-3} and 51.3 mmol m^{-3}. The concentration of PO_4^{3-} only showed seasonality in the freshwater site while concentration values decreased seawards between sites (Fig. 3 E).

The sediment at all sites was muddy with a median grain size (D50) increasing from the fresh (30.32 µm) to the marine (61.51 µm) part of the estuary (Table 1). OrgC was inversely related to grain size and porosity that decreased seawards. The sedimentary C:N ratio was highest in the brackish and lowest in the marine part of the estuary.

3.2. Pigment concentrations in the surface of the sediment

Total pigment concentration was about an order of magnitude higher in the freshwater (Fig. 4 A) compared to the other sites, and the brackish site (Fig. 4 B) had the lowest concentration. A clear summer peak was observed in freshwater site and to a lesser degree in the marine site (Fig. 4 C). In contrast, a spring peak occurred in the brackish part of the estuary. Both the brackish and marine sites had a relatively high concentration in total and in pigments associated with diatoms (Chl c, diadinoxanthin, diatoxanthin, and fucoxanthin [Reuss, 2005]) during January and February.

3.3. Fluxes across the sediment-water interface

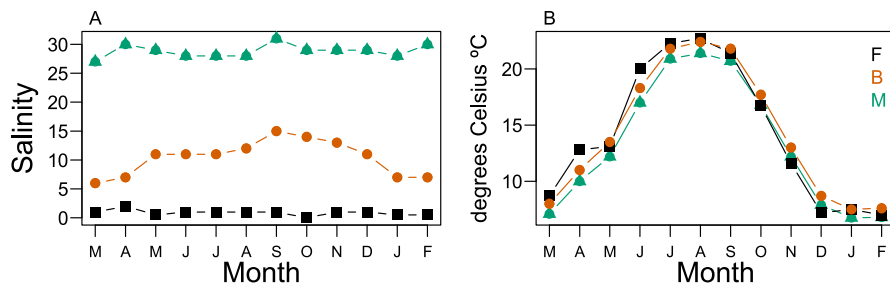Oxygen exchange rates were influenced by temperature and

Fig. 2. Salinity (A) and temperature (B) variations at freshwater (F, black squares), brackish (B, red circles) and marine (M, green triangles) stations of the Western Scheldt along the salinity gradient from March 2019 to February 2020. (For interpretation of the references to colour in this figure legend, the reader is referred to the Web version of this article.)
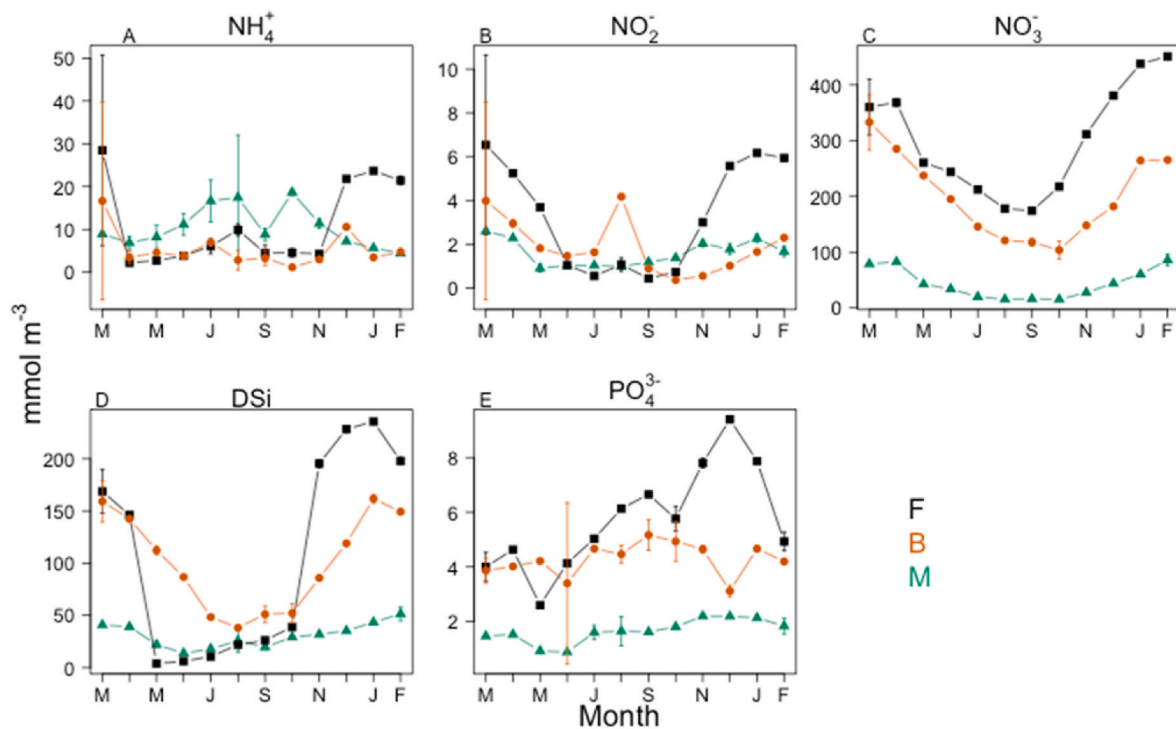

Fig. 3. Nutrient concentrations of the water column at the freshwater (F, black squares), brackish (B, red circles) and marine (M, green triangles) sites from March 2019 to February 2020. Standard deviation indicated at each point. (For interpretation of the references to colour in this figure legend, the reader is referred to the Web version of this article.)

Table 1
Yearly mean ± standard deviation of physical characteristics of the first 5 cm of the sediment in the fresh, brackish, and marine sites. Median sediment grain size (D50), organic carbon content (OrgC), porosity, and carbon: nitrogen ratio.

	Unit	Freshwater	Brackish	Marine
D50	μm	30.3 ± 6.4	48.7 ± 5.6	61.5 ± 12.2
OrgC	%	3.1 ± 0.5	1.1 ± 0.3	0.6 ± 0.1
Porosity*	–	0.8 ± 0.2	0.6 ± 0.2	0.5 ± 0.1
C:N	mol:mol	11.3 ± 0.5	13.2 ± 1.2	8.7 ± 0.9

therefore varied seasonally at all stations, peaking in the summer with a maximum of 131.4 mmol m^{-2} d^{-1} in the marine site (Fig. 5 A). The freshwater and brackish sites showed a similar average O$_2$ exchange rate (38.26 and 43.02 mmol m^{-2} d^{-1}, respectively) which was around 40% lower than in the marine part of the estuary (66.1 mmol m^{-2} d^{-1}). Interestingly, the dependence of these rates to temperature, given by Q$_{10}$ values, was lower in the freshwater site (2.55) and higher and similar in the brackish (3.06) and marine (3.01) sites. The freshwater and marine

sites had a similar efflux of NH$_4^+$ that peaked in August (~12 mmol m^{-2} d^{-1}) and appeared directly related to temperature (Fig. 5 B). While the marine site had an efflux of NH$_4^+$ throughout the year, the freshwater site showed an ammonium efflux only in spring to autumn and an influx in winter. The flux of NH$_4^+$ observed in the brackish site always fluctuated around zero and did not appear to be affected by seasonal changes in temperature. The flux of NO$_2^-$ in the freshwater site changed seasonally (Fig. 5 C) with an efflux in the warmer period of the year, and an influx in the colder period, while the flux observed in the brackish site fluctuated around zero and was a perpetual efflux in the marine site. All sites displayed an influx of NO$_3^-$ throughout the year (Fig. 5 D), with fluxes decreasing with higher salinity. A similar efflux of DSi was observed in the freshwater and brackish site (Fig. 5 E). Nevertheless, the brackish site showed an influx during the winter and spring that was not observed in the freshwater site. The DSi efflux in the marine site was highest in August at 14.0 mmol m^{-2} d^{-1}. Overall, the freshwater area exhibited an influx of phosphate with a small efflux observed from August to October (Fig. 5 F), whilst the brackish and marine sites showed an efflux of PO$_4^{3-}$ that peaked in the summer, with a small influx during the cooler months.
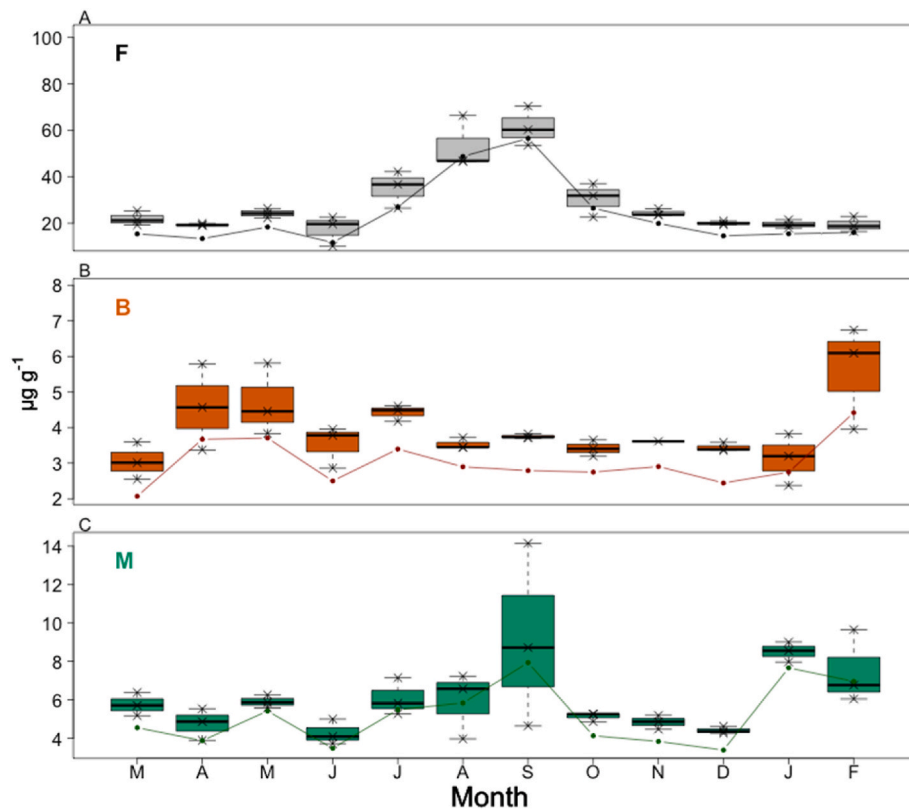
Fig. 4. Boxplot of seasonal concentrations of all pigments (Alloxanthin, carotene b, Chlorophylidae a, Chl a, Chl b, Chl c, diadinoxanthin, diatoxanthin, dinoxanthin, fucoxanthin, 19'-hexanoyloxyfucoxanthin, lutein, Mg-2,4-divinyl pheoporphyrin, neoxanthin, peridin, prasinoxanthin, violaxanthin, and zeaxanthin), and line representing the mean of pigments associated to diatoms (Chl c, diadinoxanthin, diatoxanthin, and fucoxanthin [Reuss, 2005]).
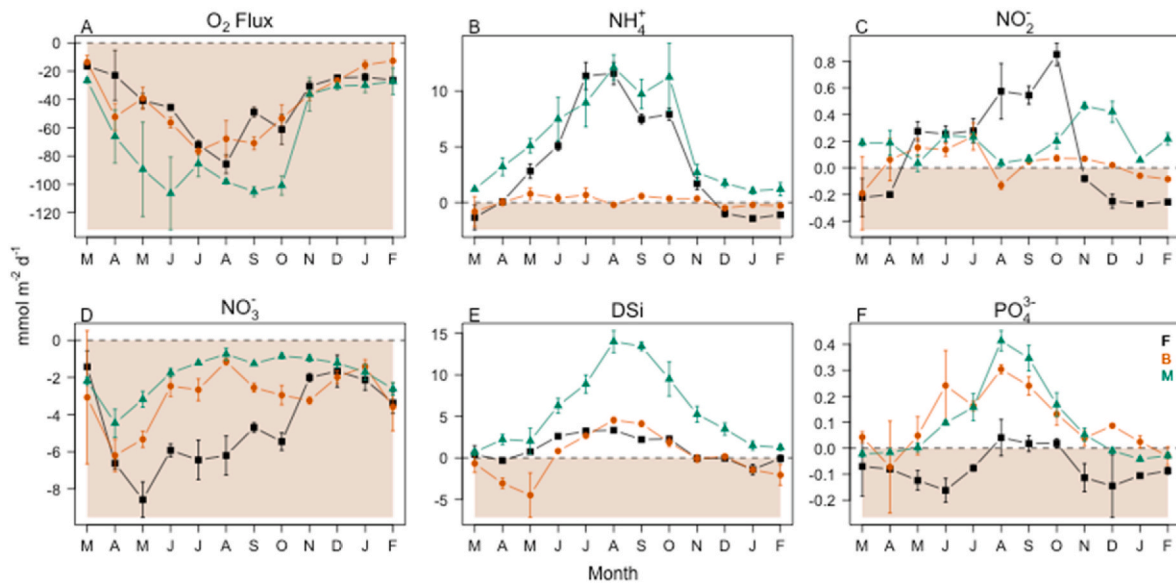

Fig. 5. Mean ± standard deviation of O_2 and nutrient fluxes. A negative flux indicates a net nutrient flux from the water column into the sediment (shaded area). Months from March 2019 to February 2020.

The yearly averaged fluxes per site (Fig. 6) clearly show that i) the freshwater site had a net influx of both DIN (1.62 mmol m^{-2} d^{-1}) and DIP (0.07 mmol m^{-2} d^{-1}), ii) the brackish site exhibited a net influx of DIN (2.84 mmol m^{-2} d^{-1}), but a net efflux of phosphate (0.1 mmol m^{-2} d^{-1}), and iii) the marine site had a net efflux of both DIN (3.83 mmol m^{-2} d^{-1}) and DIP (0.09 mmol m^{-2} d^{-1}). There was an efflux of dissolved silicate at all sites, but mostly in the marine site (5.71 mmol m^{-2} d^{-1}).

3.4. Porewater nutrients

Porewater NH_4^+ was highest at the freshwater site (Fig. 7 A) with the average concentration in the deepest layer (14 cm) being about three times as high (720 mmol m^{-3}) than in the brackish and marine sites. In these two latter sites, the general shape of NH_4^+ profiles was different with the marine site exhibiting a more accumulation with depth, but the
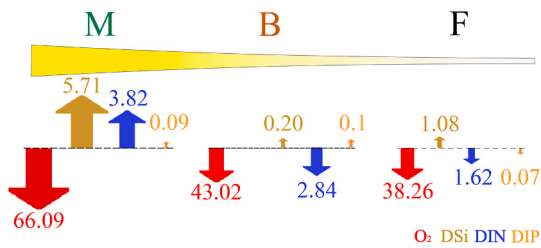
Fig. 6. Average daily fluxes (mmol m^{-2} d^{-1}) of oxygen (O$_2$) in red, dissolved silicate (DSi) in brown, dissolved inorganic nitrogen (DIN) in blue, and dissolved inorganic phosphate (DIP) in orange for the three study sites (freshwater, F; brackish, B; and marine, M). Yellow funnel shape represents the WS and its increasing salinity gradient. The dotted lines represent the sediment-water interface. Arrows pointing down indicate an influx, arrows pointing up an efflux. Image created with Adobe® Photoshop® (23.0.2 release). (For interpretation of the references to colour in this figure legend, the reader is referred to the Web version of this article.)

average concentration of the deepest layer (14 cm) was very similar (Fig. 7 F and K), reaching around 200 mmol m^{-3}. The profiles of NO$_2^-$ and NO$_3^-$ decreased over depth at all sites. The highest concentration of porewater DSi was observed in the freshwater (Fig. 7 D) (601 mmol m^{-3}) and brackish (Fig. 7 I) (560 mmol m^{-3}) sites. The concentration of PO$_4^{3-}$ was greater in the brackish site (Fig. 7 J) and lowest in the marine site (Fig. 7 O).

Based on temperature differences, we designated a cooler period, from November to May (9.5 ± 2.5 °C) and a warmer period from June to October (20.1 ± 2.2 °C). Seasonality affected the concentration of the nutrients NH$_4^+$, Dsi, and PO$_4^{3-}$ (Fig. 7 A, D, E, F, I, J, K, N and O boxplots) resulting in a higher concentration during the warmer months; this effect was greater in the deeper layers of the sediment. The opposite occurred for NO$_2^-$ and NO$_3^-$ (Fig. 7 B, C, G, H, L and M boxplots) when higher concentrations were observed in the cooler period.

3.5. Nutrient ratios

DIN:DIP ratios (Table 2) in the water column (60) of the freshwater site exceeded the Redfield N:P ratio (16:1) almost fourfold, while the obtained DSi: DIP ratio (18) was very close to Redfield (15:1). The DIN:DIP ratio of the water column decreased towards the marine site (36), although remaining well above Redfield, while the DSi: DIP ratio did not change much. In contrast, the sediment average DIN: DIP and DSi: DIP ratios in the pore water were lower than Redfield at all sites.

4. Discussion

Remineralization of OM and early diagenetic processes occurring along the WS estuary show spatial and temporal differences attributable to physical (e.g. temperature), chemical (e.g. salinity, bottom water nutrient concentrations) and biological factors (e.g. algal production). Furthermore, the WS is an example of a restored system where after the implementation of water quality improvement policies the system recovered from hypereutrophication with water column anoxia to a year-round oxic water column.

4.1. Physical characteristics of the water column and the sediment

Salinity fluctuations due to riverine discharge only prevailed in the brackish site, while seasonal temperature variations affected processes in all sites (Fig. 2). The concentration of nutrients in the water column of the WS was consistently higher in the freshwater portion of the estuary, and decreased with increasing salinity, as previously reported for the area (Andersson et al., 2006; Brion et al., 2008; Chen et al., 2007; Middelburg and Nieuwenhuize, 2000; Soetaert et al., 2006). DIN:DIP ratios exceeding Redfield (Table 2) suggested DIP limitation of primary

production in the water column for the entire WS. The DSi: DIP ratio was close to the Redfield ratio for diatoms and thus no DSi limitation was detected. A similar observation for this system was reported by Soetaert et al. (2006).

Despite the potential limitation of P based on nutrient ratios, the concentration of PO$_4^{3-}$ in the water column of the whole estuary was high (>1 mmol m^{-3}), and therefore it is unlikely that phosphate was the factor limiting primary production. Instead, it has been reported that the Western Scheldt primary production is limited by light and not by nutrients (Kromkamp and Peene, 1995; Van den Meersche et al., 2011).

The OrgC content of the sediment was highest in the freshwater part of the estuary (around 3%) and decreased downstream (1% in the brackish, 0.5% in the marine site). The C:N ratio of the sedimentary material, an indication of the OM degradability, was high in both the freshwater (11) and brackish (13) sites (Table 1). This is probably reflecting the input of refractory OM from allochthonous origin such as detritus derived from terrestrial sources (Boynton and Kemp, 1985; Hopkinson et al., 1999) or the vegetation, reed *Phragmites* sp., surrounding these areas (Struyf et al., 2005a). Allochthonous OM is by nature less degradable than autochthonous OM (Soetaert et al., 2006). A similar dominance of allochthonous and terrestrial OM upstream has been reported by Van den Meersche et al. (2009). In contrast, the low C:N ratio at the marine site indicated a greater proportion of autochthonous OM and higher degradability of OrgC possibly of algal origin e.g. diatoms (Struyf et al., 2005a).

An important source of autochthonous production in intertidal flats comes from microphytobenthos (Middelburg et al., 2000; Underwood and Kromkamp, 1999). Seasonality in microphytobenthos production was most pronounced in the freshwater site, which had the highest summer peak, while both the marine and brackish site showed a clear winter peak (January and February) (Fig. 4) possibly related to lower grazing of microphytobenthos. Photosynthetic pigments varied seasonally by only a factor 2 to 3 between summer and winter indicating a relatively steady microphytobenthic production. This has been reported as typical of microphytobenthic communities as opposed to phytoplankton production with drastic seasonal fluctuations (Terai et al., 2000).

The highest pigment concentrations were observed in the freshwater site; in contrast, they were an order of magnitude lower in the brackish site and slightly increased again towards the marine site. Similar observations have been reported for this system in the 90's (Kromkamp and Peene, 1995; Soetaert et al., 1994a) and in 2016 (Maris and Meire, 2017). Brackish regions are characterised by a transition from fresh to marine species and experience more prominent salinity fluctuations (Fig. 2 A), which could explain the lower Chl a concentration detected in this part of the estuary (Kromkamp and Peene, 1995; Soetaert et al., 1994a). The fluctuation in phytopigment concentrations was driven by diatoms (Fig. 4) which dominate the microphytobenthic community in the WS and have an increasing contribution to the community composition from upstream to downstream areas (Kromkamp and Peene, 1995; Maris and Meire, 2017; Muylaert et al., 2002).

4.2. Sediment respiration

The fate of OM in sediments is to be mineralized and recycled by biogeochemical processes, or to be buried over longer timescales. Daily sediment respiration rates (yearly average) in the dark increased from 38.3 mmol m^{-2} d^{-1} in the freshwater to 66.1 mmol m^{-2} d^{-1} in the marine site (Fig. 5 A), indicating a higher benthic activity towards the mouth of the estuary. While in theory, both higher temperature and OM availability (see algal concentrations in Fig. 4) in summer may be responsible for the elevated respiration rates, no relationship was found between the respiration rates and Chl a concentration at any site. Instead, the seasonality of respiration closely mirrored seasonal changes in temperature. Temperature, rather than OM availability, seems to be the best descriptor of sediment respiration in the WS, as also observed in
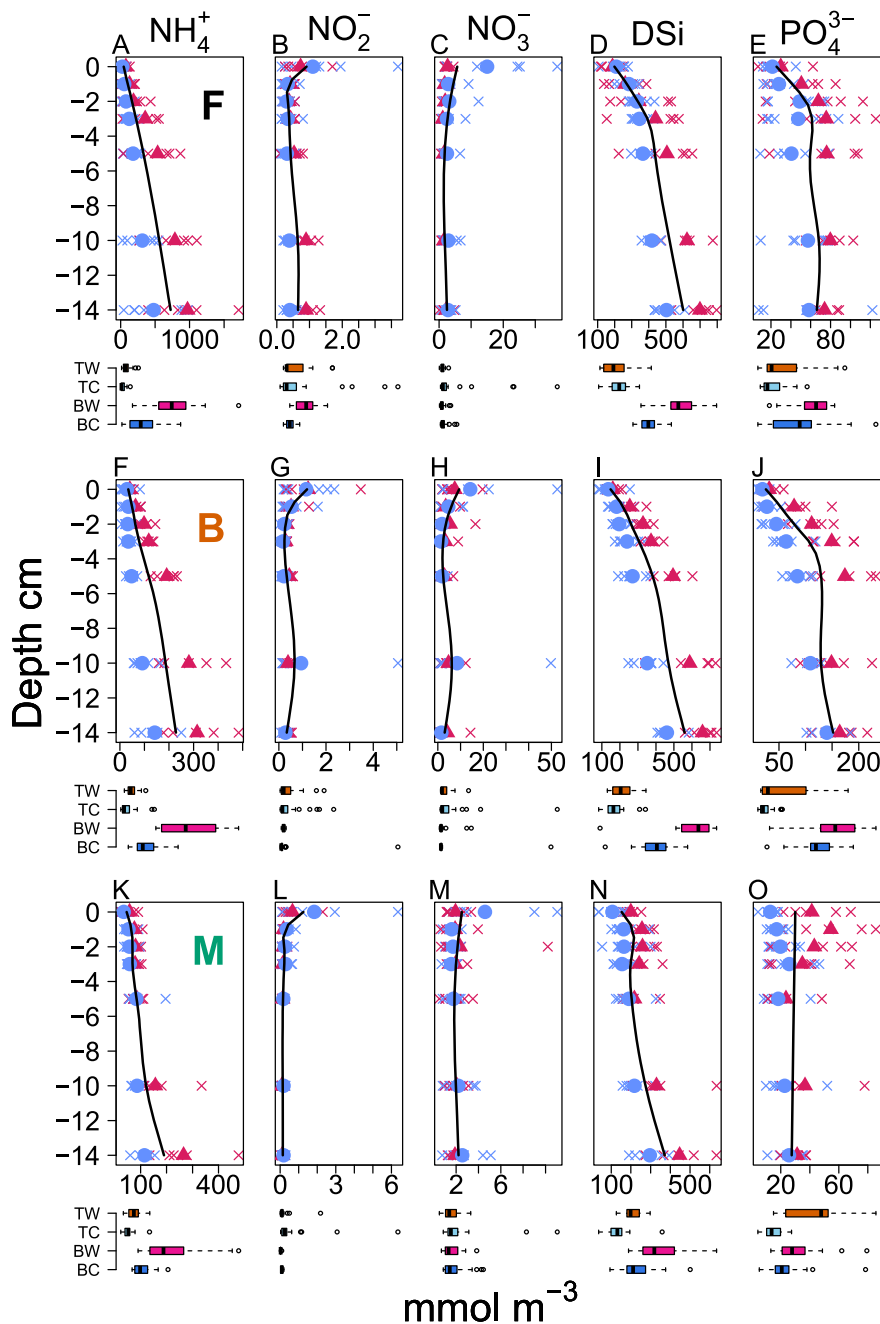
Fig. 7. Porewater profiles of the freshwater (F), brackish (B) and marine (M) sites, smoothed by means of a cubic spline of the yearly mean (black line). Warmer months (June to October) are represented with red triangles (mean per layer) and red crosses (average per month). Cooler months (March to May and November 2019 to February 2020) are shown with blue circles (mean per layer) and blue crosses (average per month). Note x-scale differences between sites. Boxplots show the comparison of values in the top 1 cm (TC: Top cool and TW: top warm)) and 10–14 cm (BC: bottom cool and BW: bottom warm) layers. (For interpretation of the references to colour in this figure legend, the reader is referred to the Web version of this article.)

Table 2
Yearly averaged molar ratios of DIN: DIP and DSi: DIP in the water column and porewater.

Site	Water column		Pore water	
	DIN: DIP	DSi: DIP	DIN: DIP	DSi: DIP
Fresh water	60	18	6	12
Brackish	49	24	2	5
Marine	36	19	4	10

other estuaries (Hopkinson et al., 1999; Jørgensen and Sørensen, 1985).

The relationship between respiration and temperature was well described with an exponential, so-called Q_{10} relationship. The Q_{10} values, around 3 in the brackish and marine sites indicate a tripling of respiration for an increase in temperature of 10°; the value in the freshwater (2.5) is closer to the theoretical value of 2. The obtained Q_{10} values are important parameters that quantify the dependence of OM degradation to temperature; and they could be used in models speculating on the effect of rising temperatures on biogeochemical processes in the estuary.

4.3. Porewater nutrients

The remineralization of OM releases bioavailable nutrients that can be temporarily stored in pore water, transformed within the sediment, or released into the overlying water column (Herbert, 1999). The shape of the nutrient profiles is influenced by i) the rate at which OM is transported deeper into the sediment (either by advection, mixing, (bio) diffusion and bioturbation), ii) the reactivity of the organic matter (decay products of highly reactive particles do not reach large depths),

iii) the intensity of mineralization or dissolution and iv) temperature, which directly affects bacterial mediated processes (e.g. respiration and remineralization) (De Borger et al., 2021). In brief, the nutrients released in the upper layers of the sediment can diffuse into the water column, but those released by dissolution and decay of OM at greater depth cause an increase in the concentration of nutrients such as NH_4^+, DSi, and –to a lesser extent– PO_4^{3-} (Fig. 7).

All sites exhibited a gradual increase in the concentration of ammonium (Fig. 7 A, F and K) and a decrease in the concentration of NO_2^- and NO_3^- (Fig. 7 B, C, G, H, L and M). These dynamics are explained by the release of NH_4^+ from OM mineralization and its conversion to NO_2^- and NO_3^- via nitrification. In deeper layers of the sediment NH_4^+ accumulates as it is released from OM, and the concentration of NO_2^- and NO_3^- decreases as a consequence of net consumption likely by anammox and denitrification.

The fresh and brackish sites (Fig. 7 D and I) showed a gradual increase in the concentration of DSi. These sites are close to a salt marsh populated by reed (*Phragmites australis)*, which accumulates BSi in its tissues in the form of phytoliths (Struyf et al., 2005b). When reed-derived OM is buried into the sediment, the BSi (from phytoliths) dissolves to form DSi (Struyf et al., 2005b) causing its accumulation at depth. In contrast, the DSi profile in the marine site (Fig. 7 N) showed a rapid increase in the upper 5 cm indicating that mineralization and dissolution were restricted to the uppermost layers. This suggests an alternative source of BSi to reed was present in this site, most likely the siliceous frustules of benthic diatoms (Struyf et al., 2005b). Diatom frustules exhibit higher dissolution rates than reed phytoliths (Loucaide et al., 2008) which could result in the rapid increase in DSi concentration observed in this site. The pigment analyses (Fig. 4) shows that diatoms are an important microphytobenthic group at all sites (Maris and Meire, 2017). However, the green algae *Euglena* sp., which does not accumulate BSi (Barsanti and Gualtieri, 2020), was dominant in the freshwater site. The main sources of DSi in the WS intertidal sediments are diatom frustules in all sites, and reed phytoliths in the freshwater and brackish sites (Struyf et al., 2005b).

The higher concentration of PO_4^{3-} observed in freshwater and brackish sediments (Fig. 7 E and J) may be associated with the sorption of PO_4^{3-} to iron oxides that is promoted in areas with lower salinities (Jordan et al., 2008; Slomp et al., 1996). While the gradual increase in PO_4^{3-} concentration over depth could either result from the P-shuttle transporting iron oxides downwards and desorbing PO_4^{3-} into the anoxic layer as the iron oxides dissolve or from OM degradation releasing PO_4^{3-} (Caraco et al., 1990; Jordan et al., 2008; Slomp et al., 1996). Moreover, high levels of DSi in the pore water, like observed in these sites (Fig. 7 D and I), enhance sorption of PO_4^{3-} to iron oxides and may increase the quantity of PO_4^{3-} entering the sediment and desorbing at depth (Mayer and Jarrell, 2000). In contrast, the marine area exhibited a lower concentration of pore water PO_4^{3-} (Fig. 6 E, J and O) which may be explained by the higher salinity as it reduces sorption of PO_4^{3-} (Caraco et al., 1990; Jordan et al., 2008) and decreases the efficiency of the P-shuttle (Jordan et al., 2008). In areas with a large sulphate concentration (higher salinity), the sulphide (HS^-) produced during sulphate reduction binds to Fe(II) as iron sulphide thereby preventing the formation of $FeOOH$-PO_4^{3-} compounds; and promoting the desorption of PO_4^{3-} from $FeOOH$ and its release into the water column (Caraco et al., 1990; Jordan et al., 2008).

All sites had sedimentary DIN:DIP ratios that were significantly below Redfield, suggesting that sediments either retained more PO_4^{3-} than DIN and/or had more efficient N compared to P removal processes. This was most prominent at the brackish site, where the DIN:DIP ratio was as low as 1.4 mol: mol at 14 cm (Appendix 1), whereas the Redfield ratio is 16. The proportion of DIN relative to DIP being much lower than the N:P ratio of the original organic matter may be a consequence of the build-up of PO_4^{3-} due to desorption and release at depth, but also of the absence of an equivalent mechanism capturing DIN in the upper layers of the sediment and releasing it at depth. Nevertheless, a lower than

Redfield N:P ratio may also arise when the DIN is more efficiently removed from the sediment than DIP through coupled nitrification-denitrification.

4.4. Porewater seasonality

The effect of temperature on the concentration of pore water nutrients was detected up to 14 cm depth, however, fluctuations in intertidal muddy sediments have been observed up to 5 m deep (Beck et al., 2008; Harrison and Phizacklea, 1987). The concentration of NH_4^+ at all sites doubled during the warmer months (Fig. 7 A, F and K), possibly as a result of higher decomposition and regeneration rates (Magni and Montani, 2006; Middelburg et al., 1995b) as evidenced by Q_{10} values. In contrast, the difference in the concentration of NO_2^- and NO_3^- between the warm and cool period was more subtle and seemed reversed with lower concentrations in warmer months versus higher in cooler months. While this might suggest a larger net consumption at higher temperature possibly associated with increased denitrification, this may be unlikely. Rather, a higher bottom water concentration of NO_2^- and NO_3^- in the cooler months (Fig. 3 B and C) may have directly influenced their concentration in pore waters (Kemp et al., 1990; Magni and Montani, 2006; Zhang and Huang, 2011) and a deeper O_2 penetration depth in the winter (Sagemann et al., 1996) together with lower OM remineralization rates may have facilitated nitrification, and thus the observed increase in concentration.

The concentration of DSi increased by more than 50% (Fig. 7 D, I and N) in the hotter months. Likely resulting from the increased dissolution of BSi with higher temperature (Kamatani, 1982; Lawson et al., 1978; Struyf et al., 2005b). Similar observations on increasing concentrations of NH_4^+ and DSi with temperature have been reported in other systems (e.g. Kemp et al., 1990; Magni and Montani, 2006; Middelburg et al., 1995a; Sagemann et al., 1996).

Phosphate concentrations were also higher in the warm compared to the cool months, but here the difference appeared to be greatest at intermediate depths (~5 cm) in the freshwater and brackish site, while in the marine site, the fluctuations remained in the sediment surface (~2 cm). Possibly, the effect of temperature was less prominent in the surface sediment because higher temperature increased bioturbation activity and transport of OM and PO_4^{3-} to deeper sediments via the P-shuttle, which together with higher OM mineralization rates caused the release of PO_4^{3-} at depth. Nevertheless, a higher temperature can also enhance sorption of PO_4^{3-} onto sediment particles (Zhang and Huang, 2011), but salinity may be a controlling factor.

4.5. Nutrient fluxes

The summer peak observed for the flux of NH_4^+ in the fresh and marine sites likely resulted from higher regeneration rates and OM decomposition (Magni and Montani, 2006; Middelburg et al., 1995b). The range of NH_4^+ fluxes observed in the WS was within values reported for other temperate estuaries (0.67–23.47 mmol m^{-2} d^{-1}) (Boynton and Kemp, 1985; Magalhães et al., 2002; Thouzeau et al., 2007). Unexpectedly, the ammonium flux at the brackish site was close to zero (Fig. 5 B), an indication of high NH_4^+ consumption by nitrification in the sediments (Magalhães et al., 2002; Middelburg and Nieuwenhuize, 2000; Rysgaard et al., 1999). It is unlikely that microphytobenthos growth would cause such a trend since i) the Chl a concentration in the brackish part was the lowest of all sites and ii) the yearly pigment fluctuation was similar to that of the marine site where there was a clear efflux during the summer. This, together with the large influx of nitrate (Fig. 5 D) is evidence of the substantial removal of bioavailable nitrogen due to denitrification in the brackish site. A year-round influx of NO_3^- has also been reported in the Douro River estuary (Magalhães et al., 2002), but this is different in other estuaries (Cowan et al., 1996; Thouzeau et al., 2007).

Although both the freshwater and marine sites had a year-round

efflux of DSi, the brackish site showed a distinctive influx of DSi in the spring and winter (Fig. 5 E), concurrent with the pigment peaks observed at that time (Fig. 4 B). It is therefore possible that this influx was caused by the uptake of DSi by diatoms (Hopkinson et al., 1999).

The flux of PO_4^{3-} in the freshwater site was generally directed into the sediment (Fig. 5 F), except for the three warmest months (August–October) when the sediment was most anoxic, and desorption was promoted. It is unlikely that microphytobenthos uptake affected the influx of PO_4^{3-} in the winter since the pigment concentration was lowest in that period. It therefore seems that sorption was the principal mechanism of P loss in the freshwater site. A similar PO_4^{3-} influx has been observed in other freshwater sediments (Hopkinson et al., 1999), while an efflux, like that of the brackish and marine sites, has also been reported for saline sediments (Cowan et al., 1996; Thouzeau et al., 2007).

The impact of temperature on sediment biogeochemistry was also clear from the nutrient fluxes (Fig. 5) that showed greater effluxes with higher temperatures for NH_4^+ (freshwater and marine site), NO_2^- (marine), PO_4^{3-} (brackish and marine) and DSi (all stations). In contrast, there was an influx of NO_3^- that consistently peaked in the spring rather than in summer (Fig. 5 D) similar trends have been discussed in Kemp et al. (1990).

4.6. Nutrient retention of intertidal sediments

To understand the role of intertidal sediments in the nutrient retention capacity of the Western Scheldt estuary, the nutrient budgets for the fresh, brackish, and marine sites obtained from this study were used to estimate the nutrient budgets for the whole intertidal area of the WS. This approach was based on that of Middelburg et al. (1996) and assumes that the mineralization rates obtained in the fresh, brackish, and marine sites are representative of each zone.

The calculation was based on the yearly-averaged nutrient fluxes (Fig. 6) of DIN ($NH_4^+ + NO_2^- + NO_3^-$) and PO_4^{3-}. These fluxes were converted to integrated rates and compared to inputs of total nitrogen ($\sim$14,000 t N y^{-1}) and total phosphate ($\sim$1400 t P y^{-1}) from tributaries (Scheldt, Dender, and Rupel rivers), as estimated from riverine water discharge (average 78 m^3 s^{-1}) and yearly averaged nutrient concentrations (obtained from Flanders Environment Agency, n.d.). The total area of the freshwater intertidal sediments (3413 km^2) was taken from Struyf et al. (2004), and the area of brackish (28,366 km^2) and marine (50,271 km^2) intertidal sediments was extracted from recent bathymetry data between −2 and 2 m NAP. To account for the tidal regime of intertidal sediments (12 h emersion), the fluxes were multiplied by 0.5 (Soetaert et al., 1992).

Assuming an O:C ratio in mineralization rate of 1, the intertidal sediments remineralized a total of 10,000 t C y^{-1} with 97% of mineralization occurring in the brackish (26%) and marine (71%) sections of the estuary. This illustrates that, because of their lower mineralization and relatively small surface area, the contribution of freshwater sediments to estuarine remineralization was negligible (only 3%). The estimated total mineralization was lower than that estimated for the beginning of the 1990's (16,000 t C y^{-1}, Middelburg et al., [1996]), but was comparable. The difference could be attributed to changes in the total surface area of intertidal sediments from the 1990's, to the consideration of the tidal regime in our calculation, or to the diminution of nutrients and OM discharging into the WS because of water quality management efforts.

OM remineralization and fluxes of DIN and phosphate accounted for a total of $\sim$1500 t N y^{-1} and $\sim$200 t P y^{-1}, and 11% of nitrogen and 15% of phosphorus from riverine input being removed or retained within the estuary (e.g. by nitrification, denitrification, sorption or burial). The function of each section and their contribution to nutrients retention resembled a three-step filter. The freshwater area functions as a first barrier for nutrients reaching the estuary, which despite its small area, was a sink of inorganic P (9.0 t P y^{-1}) and N (61.9 t N y^{-1}), as evidenced by the high influxes (Fig. 6). In contrast, the brackish and marine areas,

although with a comparatively less efficient influx per meter squared than the freshwater site, contributed greatly to nutrient retention because of their greater surface area. Nutrient filtration by intertidal sediments is therefore evidenced as an important mechanism decreasing the quantity of nutrients reaching the North Sea and buffering against eutrophication (Sagemann et al., 1996). Similar findings on the importance of intertidal sediments for estuarine nutrient retention have been reported for other estuaries (Jickells et al., 2000; Liu et al., 2020; Magalhães et al., 2002).

4.7. Historical overview of the state of the Western Scheldt estuary

The WS has a history of anthropogenic influence that has caused eutrophication and decreased water quality that peaked during the 1970's (Soetaert et al., 2006; Wollast and Peters, 1978). Since then, sanitation schemes to restore ecosystem function and limit the influx of pollutants, raw sewage, and fertilizers have been implemented around the watershed, substantially ameliorating the water quality of the estuary (Brion et al., 2015; Soetaert and Herman, 1995a). For example, the opening of the Brussels-North wastewater treatment plant in 2007, reduced nutrient loads and improved the oxygen saturation of the main tributary of the WS, the Rupel river (Brion et al., 2015). However, there has not been an assessment of the long-term effect of the wastewater treatment plant on the concentration of nutrients in the WS since its implementation.

A comparison of the nutrient concentrations measured in the water column with values reported in early 2000's (Soetaert et al., 2006), demonstrates significant changes in the water quality of the WS. Soetaert et al. (2006) already observed an improvement in the water quality of the WS from 1970 to 2000 regarding lower concentrations of NH_4^+, NO_2^-, DIP and DSi. While the concentration of NO_3^- and PO_4^{3-} measured in 2019–2020 has remained similar to values reported in 2002, the concentrations of the other nutrients were different to those observed in the beginning of the century. In the early 2000's there was a prominent seaward decrease in NH_4^+ concentration from the freshwater ($\sim$80 mmol m^{-3}) to the marine ($\sim$6 mmol m^{-3}) sector (Soetaert et al., 2006). Currently, the freshwater (11 mmol m^{-3}), marine (10 mmol m^{-3}) and brackish sites (5.4 mmol m^{-3}) have rather similar NH_4^+ concentrations. The largest changes since 2000, are observed in the freshwater site concerning NO_2^- and DSi with the concentration of NO_2^- decreasing from 14 mmol m^{-3} (Soetaert et al., 2006) to 3 mmol m^{-3} currently, and that of DSi decreased from $\sim$190 mmol m^{-3} (Soetaert et al., 2006) to $\sim$100 mmol m^{-3}. The reduction of nitrite in the freshwater site might be associated to the prevalence of oxic conditions in the water column that have promoted nitrification (Cox et al., 2009; Soetaert and Herman, 1995a; Van Damme et al., 2005). In contrast, the NO_2^- concentration at the marine site has remained unchanged, while the concentration of DSi has doubled.

The river discharge has increased over time from 70 m^3 s^{-1} in 2000 (Struyf et al., 2004) to a long-term (1971–2015) mean of 120 m^3 s^{-1} in 2015 (Wang et al., 2019). A higher discharge dilutes nutrient concentrations and would cause lower concentration values, despite the total nutrient loading reaching the WS (Struyf et al., 2004) being unchanged. However, for the period of our sampling, we obtained average discharge velocities of 78 m^3 s^{-1}, so that dilution can be ruled out as an important factor explaining the decrease in concentration. It is more likely that the reduction in nutrient concentrations (NH_4^+, NO_2^-, and DSi) reflects the recovery process from eutrophication caused by better sanitation policies such as the implementation of wastewater treatment upstream.

In summary, the processes near the sediment-water interface in estuarine systems depend just as much on seasonality as on the physicochemical characteristics of the study site. Water column properties cause freshwater sites to act as an efficient trap of P and N, while the brackish sites efficiently remove DIN. Temperature was the principal factor affecting overall nutrient fluxes and pore water concentrations of NH_4^+, DSi and PO_4^{3-} while those of NO_2^-, NO_3^- were mostly influenced by

bottom water concentrations. The information obtained in the present study adds to our understanding of the complexity of biogeochemical interactions in estuaries and indicates an important role of intertidal sediments for the biogeochemistry of estuarine systems and adjacent seas. It is relevant for researchers addressing the effects of water treatment policies on estuarine biogeochemistry, the environmental impact of intertidal ecosystem losses or the effects of climate change related stressors on benthic biogeochemistry, among others. Moreover, a positive relationship was recognised between policy and ecosystem functionality restoration where the implementation of policy aimed at improving water quality resulted in sediments regaining their nutrient filter functionality which also ameliorated water quality. This information is important for policy makers and managers as it places emphasis in restoring ecosystem functionality.

CRediT authorship contribution statement

Dunia Rios-Yunes: Writing – review & editing, Writing – original draft, Visualization, Validation, Methodology, Formal analysis, Data curation, Conceptualization. **Justin C. Tiano:** Writing – review & editing, Resources, Conceptualization. **Dick van Oevelen:** Writing – review & editing, Supervision, Conceptualization. **Jeroen van Dalen:** Validation, Resources, Investigation. **Karline Soetaert:** Writing – review & editing, Validation, Supervision, Software, Project administration, Methodology, Formal analysis, Conceptualization.

Declaration of competing interest

The authors declare that they have no known competing financial interests or personal relationships that could have appeared to influence the work reported in this paper.

Data availability

Data will be made available on request.

Appendix A. Supplementary data

Supplementary data to this article can be found online at https://doi.org/10.1016/j.ecss.2023.108227.

References

Andersson, M., Brion, N., Middelburg, J., 2006. Comparison of nitrifier activity versus growth in the Scheldt estuary - a turbid, tidal estuary in northern Europe. Aquat. Microb. Ecol. 42, 149–158. https://doi.org/10.3354/ame042149.

Arndt, S., Jørgensen, B.B., LaRowe, D.E., Middelburg, J.J., Pancost, R.D., Regnier, P., 2013. Quantifying the degradation of organic matter in marine sediments: a review and synthesis. Earth Sci. Rev. 123, 53–86. https://doi.org/10.1016/j.earscirev.2013.02.008.

Arndt, S., Regnier, P., Vanderborght, J.-P., 2009. Seasonally-resolved nutrient export fluxes and filtering capacities in a macrotidal estuary. J. Mar. Syst. 78, 42–58. https://doi.org/10.1016/j.jmarsys.2009.02.008.

Baeyens, W., van Eck, B., Lambert, C., Wollast, R., Goeyens, L., 1997. General description of the Scheldt estuary. Hydrobiologia 366, 1–14. https://doi.org/10.1023/a:1003164009031.

Bally, G., Mesnage, V., Deloffre, J., Clarisse, O., Lafite, R., Dupont, J.-P., 2004. Chemical characterization of porewaters in an intertidal mudflat of the Seine estuary: relationship to erosion–deposition cycles. Mar. Pollut. Bull. 49, 163–173. https://doi.org/10.1016/j.marpolbul.2004.02.005.

Barsanti, L., Gualtieri, P., 2020. Anatomy of Euglena gracilis. In: Handbook of Algal Science, Technology and Medicine. Elsevier, pp. 61–70. https://doi.org/10.1016/B978-0-12-818305-2.00004-8.

Beck, M., Dellwig, O., Liebezeit, G., Schnetger, B., Brumsack, H.-J., 2008. Spatial and seasonal variations of sulphate, dissolved organic carbon, and nutrients in deep pore waters of intertidal flat sediments. Estuar. Coast Shelf Sci. 79, 307–316. https://doi.org/10.1016/j.ecss.2008.04.007.

Billen, G., Garnier, J., Rousseau, V., 2005. Nutrient fluxes and water quality in the drainage network of the Scheldt basin over the last 50 years. Hydrobiologia 540, 47–67. https://doi.org/10.1007/s10750-004-7103-1.

Boynton, W., Kemp, W., 1985. Nutrient regeneration and oxygen consumption by sediments along an estuarine salinity gradient. Mar. Ecol. Prog. Ser. 23, 45–55. https://doi.org/10.3354/meps023045.

Brion, N., Andersson, M., Elskens, M., Diaconu, C., Baeyens, W., Dehairs, F., Middelburg, J., 2008. Nitrogen cycling, retention and export in a eutrophic temperate macrotidal estuary. Mar. Ecol. Prog. Ser. 357, 87–99. https://doi.org/10.3354/meps07249.

Brion, N., Verbanck, M.A., Bauwens, W., Elskens, M., Chen, M., Servais, P., 2015. Assessing the impacts of wastewater treatment implementation on the water quality of a small urban river over the past 40 years. Environ. Sci. Pollut. Control Ser. 22, 12720–12736. https://doi.org/10.1007/s11356-015-4493-8.

Caraco, N., Cole, J., Likens, GeneE., 1990. A comparison of phosphorus immobilization in sediments of freshwater and coastal marine systems. Biogeochemistry 9, 277–290. https://doi.org/10.1007/BF00000602.

Chen, M.S., Wartel, S., Lavkulich, L.M., Baeyens, W., Goeyens, L., Brion, N., 2007. Organic matter and dissolved inorganic nitrogen distributions in estuarine muddy deposits. Aquat. Ecosys. Health Manag. 10, 69–85. https://doi.org/10.1080/14634980701211896.

Cook, P., Butler, E., Eyre, B., 2004. Carbon and nitrogen cycling on intertidal mudflats of a temperate Australian estuary. I. Benthic metabolism. Mar. Ecol. Prog. Ser. 280, 25–38. https://doi.org/10.3354/meps280025.

Cowan, J., Pennock, J., Boynton, W., 1996. Seasonal and interannual patterns of sediment-water nutrient and oxygen fluxes in Mobile Bay, Alabama (USA):regulating factors and ecological significance. Mar. Ecol. Prog. Ser. 141, 229–245. https://doi.org/10.3354/meps141229.

Cox, T.J.S., Maris, T., Soetaert, K., Conley, D.J., van Damme, S., Meire, P., Middelburg, J. J., Vos, M., Struyf, E., 2009. A macro-tidal freshwater ecosystem recovering from hypereutrophication: the Schelde case study. Biogeosciences 6, 2935–2948. https://doi.org/10.5194/bg-6-2935-2009.

De Borger, E., Braeckman, U., Soetaert, K., 2021. Rapid organic matter cycling in North Sea sediments. Continent. Shelf Res. 214, 104327 https://doi.org/10.1016/j.csr.2020.104327.

Deltares, 2013. Tidal Phenomena in the Scheldt Estuary part 2.

Fang, X., Mestdagh, S., Ysebaert, T., Moens, T., Soetaert, K., van Colen, C., 2019. Spatio-temporal variation in sediment ecosystem processes and roles of key biota in the Scheldt estuary. Estuar. Coast Shelf Sci. 222, 21–31. https://doi.org/10.1016/j.ecss.2019.04.001.

Feuillet-Girard, M., Gouleau, D., Blanchard, G., Joassard, L., 1997. Nutrient fluxes on an intertidal mudflat in Marennes-Oléron Bay, and influence of the emersion period. Aquat. Living Resour. 10, 49–58. https://doi.org/10.1051/alr:1997005.

Flanders Environment Agency, n.d. Geoloket [WWW Document]. URL http://geoloket.vmm.be/Geoviews/(accessed 10.20.21a).

Flanders Environment Agency, n.d. Flanders environment agency [WWW Document]. URL https://www.waterinfo.be/Themas#item=waterkwaliteit/fysische (parameters).

Flemish Government. Kaartencatalogus, 10.10.21. https://www.waterinfo.be/kaartencatalogus. WWW Document.

Gilbert, A., Schaafsma, M., de Nocker, L., Liekens, I., Broekx, S., 2007. Case study status report Scheldt river basin doi.org/10.1.1.713.9579.

Harrison, S.J., Phizacklea, A.P., 1987. Vertical temperature gradients in muddy intertidal sediments in the Forth estuary, Scotland1. Limnol. Oceanogr. 32, 954–963. https://doi.org/10.4319/lo.1987.32.4.0954.

Herbert, R., 1999. Nitrogen cycling in coastal marine ecosystems. FEMS Microbiol. Rev. 23, 563–590. https://doi.org/10.1016/S0168-6445(99)00022-4.

Hofmann, A.F., Soetaert, K., Middelburg, J.J., 2008. Nitrogen and carbon dynamics in the Scheldt estuary at the beginning of the 21st century; a modelling study. Biogeosci. Discuss. 5, 83–161. https://doi.org/10.5194/bgd-5-83-2008.

Hopkinson, C.S., Giblin, A.E., Tucker, J., Garritt, R.H., 1999. Benthic metabolism and nutrient cycling along an estuarine salinity gradient. Estuaries 22, 863. https://doi.org/10.2307/1353067.

Jickells, T., Andrews, J., Samways, G., Sanders, R., Malcolm, S., Sivyer, D., Parker, R., Nedwell, D., Trimmer, M., Ridgway, J., 2000. Nutrient fluxes through the Humber estuary - past, present and future. Ambio 29, 130–135. https://doi.org/10.1579/0044-7447-29.3.130.

Jordan, T.E., Cornwell, J.C., Boynton, W.R., Anderson, J.T., 2008. Changes in phosphorus biogeochemistry along an estuarine salinity gradient: the iron conveyer belt. Limnol. Oceanogr. 53, 172–184. https://doi.org/10.4319/lo.2008.53.1.0172.

Jørgensen, B., Sørensen, J., 1985. Seasonal cycles of 02, N03- and S042- reduction in estuarine sediments: the significance of an N03- reduction maximum in spring. Mar. Ecol. Prog. Ser. 24, 65–74. https://doi.org/10.3354/meps024065.

Kamatani, A., 1982. Dissolution rates of silica from diatoms decomposing at various temperatures. Mar. Biol. 68, 91–96. https://doi.org/10.1007/BF00393146.

Kemp, W.M., Sampou, P., Caffrey, J., Mayer, M., Henriksen, K., Boynton, W.R., 1990. Ammonium recycling versus denitrification in Chesapeake Bay sediments. Limnol. Oceanogr. 35, 1545–1563. https://doi.org/10.4319/lo.1990.35.7.1545.

Khalil, K., Laverman, A.M., Raimonet, M., Rabouille, C., 2018. Importance of nitrate reduction in benthic carbon mineralization in two eutrophic estuaries: modeling, observations and laboratory experiments. Mar. Chem. 199, 24–36. https://doi.org/10.1016/j.marchem.2018.01.004.

Kromkamp, J., Peene, J., 1995. Possibility of net phytoplankton primary production in the turbid Schelde Estuary (SW Netherlands). Mar. Ecol. Prog. Ser. 121, 249–259. https://doi.org/10.3354/meps121249.

Kuijper, K., Lescinski, J., 2013. Data-analysis water levels, bathymetry Western Scheldt. https://www.vnsc.eu/uploads/2014/02/g-5-data-analysis-water-levels-bathymetry-western-scheldt-v2-0.pdf.

Lawson, D.S., Hurd, D.C., Pankratz, H.S., 1978. Silica dissolution rates of decomposing phytoplankton assemblages at various temperatures. Am. J. Sci. 278, 1373–1393. https://doi.org/10.2475/ajs.278.10.1373.

Lessin, G., Artioli, Y., Almroth-Rosell, E., Blackford, J.C., Dale, A.W., Glud, R.N., Middelburg, J.J., Pastres, R., Queirós, A.M., Rabouille, C., Regnier, P., Soetaert, K., Solidoro, C., Stephens, N., Yakushev, E., 2018. Modelling marine sediment biogeochemistry: current knowledge gaps, challenges, and some methodological advice for advancement. Front. Mar. Sci. 5, 1–8. https://doi.org/10.3389/fmars.2018.00019.

Liu, C., Hou, L., Liu, M., Zheng, Y., Yin, G., Dong, H., Liang, X., Li, X., Gao, D., Zhang, Z., 2020. In situ nitrogen removal processes in intertidal wetlands of the Yangtze Estuary. J. Environ. Sci. (China) 93, 91–97. https://doi.org/10.1016/j.jes.2020.03.005.

Loucaide, S., Cappelle, P.van, Behrends, T., 2008. Dissolution of biogenic silica from land to ocean: role of salinity and pH. Limnol. Oceanogr. 53, 1614–1621. https://doi.org/10.4319/lo.2008.53.4.1614.

Magalhães, C., Bordalo, A., Wiebe, W., 2002. Temporal and spatial patterns of intertidal sediment-water nutrient and oxygen fluxes in the Douro River estuary, Portugal. Mar. Ecol. Prog. Ser. 233, 55–71. https://doi.org/10.3354/meps233055.

Magni, P., Montani, S., 2006. Seasonal patterns of pore-water nutrients, benthic chlorophyll a and sedimentary AVS in a macrobenthos-rich tidal flat. Hydrobiologia 571, 297–311. https://doi.org/10.1007/s10750-006-0242-9.

Maris, T., Meire, P., 2017. OMES rapport 2016. Onderzoek naar de gevolgen van het Sigmaplan, baggeractiviteiten en havenuitbreiding in de Zeeschelde op het milieu. Antwerpen.

Mayer, T.D., Jarrell, W.M., 2000. Phosphorus sorption during iron(II) oxidation in the presence of dissolved silica. Water Res. 34, 3949–3956. https://doi.org/10.1016/S0043-1354(00)00158-5.

Mestdagh, S., Fang, X., Soetaert, K., Ysebaert, T., Moens, T., van Colen, C., 2020. Seasonal variability in ecosystem functioning across estuarine gradients: the role of sediment communities and ecosystem processes. Mar. Environ. Res. 162, 105096 https://doi.org/10.1016/j.marenvres.2020.105096.

Middelburg, J.J., Barranguet, C., Boschker, H.T.S., Herman, P.M.J., Moens, T., Heip, C.H. R., 2000. The fate of intertidal microphytobenthos carbon: an in situ 13 C-labeling study. Limnol. Oceanogr. 45, 1224–1234. https://doi.org/10.4319/lo.2000.45.6.1224.

Middelburg, J.J., Duarte, C.M., Gattuso, J.-P., 2005. Respiration in coastal benthic communities. In: Respiration in Aquatic Ecosystems. Oxford University Press, pp. 206–224. https://doi.org/10.1093/acprof:oso/9780198527084.003.0011.

Middelburg, J.J., Klaver, G., Nieuwenhuize, J., Markusse, R.M., Vlug, T., van der Nat, F. J.W.A., 1995a. Nitrous oxide emissions from estuarine intertidal sediments. Hydrobiologia 311, 43–55. https://doi.org/10.1007/BF00008570.

Middelburg, J.J., Klaver, G., Nieuwenhuize, J., Vlug, T., 1995b. Carbon and nitrogen cycling in intertidal sediments near Doel, Scheldt Estuary. Hydrobiologia 311, 57–69. https://doi.org/10.1007/BF00008571.

Middelburg, J.J., Klaver, G., Nieuwenhuize, J., Wielemaker, A., de Haas, W., Vlug, T., Nat, J.F.W.A. van der, Haas, Wim de, Vlug, T., Nat, J.F.W.A. van der, 1996. Organic matter mineralization in intertidal sediments along an estuarine gradient. Mar. Ecol. Prog. Ser. 132, 157–168.

Middelburg, J.J., Nieuwenhuize, J., 2000. Uptake of dissolved inorganic nitrogen in turbid, tidal estuaries. Mar. Ecol. Prog. Ser. 192, 79–88. https://doi.org/10.3354/meps192079.

Mortimer, R.J.G., Krom, M.D., Watson, P.G., Frickers, P.E., Davey, J.T., Clifton, R.J., 1999. Sediment-water exchange of nutrients in the intertidal zone of the Humber estuary, UK. Mar. Pollut. Bull. 37, 261–279. https://doi.org/10.1016/S0025-326X(99)00053-3.

Muylaert, K., van Nieuwerburgh, L., Sabbe, K., Vyverman, W., 2002. Microphytobenthos communities in the freshwater tidal to brackish reaches of the Schelde estuary (Belgium). Belg. J. Bot. 135, 15–26. https://doi.org/10.2307/20794495.

Pastuszak, M., Conley, D.J., Humborg, C., Witek, Z., Sitek, S., 2008. Silicon dynamics in the oder estuary, baltic sea. J. Mar. Syst. 73, 250–262. https://doi.org/10.1016/j.jmarsys.2007.10.013.

QGIS Development Team, 2021. QGIS Geographic Information System.

R Core Team, 2020. R: A Language and Environment for Statistical Computing.

Reuss, N., 2005. Sediment Pigments as Biomarkers of Environmental Change. Ph.D. thesis. University of Copenhagen.

Rijkswaterstaat Waterinfo [WWW Document] Rijkswaterstaat, n.d.. Nutriënten en eutrofiëringsparameters-OW, 8.2.22a. https://waterinfo.rws.nl/.

Rijkswaterstaat, n.d.. National georegister, 10.15.21b. https://www.nationaalgeoregister.nl/geonetwork/srv//dut/catalog.search#/home. WWW Document]. URL.

Rysgaard, S.S., Thastum, P., Dalsgaard, T., Christensen, P.B., Sloth, N.P., Rysgaard, S.S., 1999. Effects of salinity on NH4+ adsorption capacity, nitrification, and denitrification in Danish estuarine sediments. Estuaries 22, 21. https://doi.org/10.2307/1352923.

Sagemann, J., Skowronek, F., Dahmke, A., Schulz, H.D., 1996. Pore-water response on seasonal environmental changes in intertidal sediments of the Weser Estuary, Germany. Environ. Geol. 27, 362–369. https://doi.org/10.1007/s002540050070.

Sharp, J.H., Pennock, J.R., Church, T.M., Tramontano, J.M., Cifuentes, L.A., 1984. The estuarine interaction of nutrients, organics, and metals: a case study in the Delaware estuary. In: The Estuary as a Filter. Elsevier, pp. 241–258. https://doi.org/10.1016/B978-0-12-405070-9.50017-7.

Slomp, C.P., Epping, E.H.G., Helder, W., Raaphorst, W. van, 1996. A key role for iron-bound phosphorus in authigenic apatite formation in North Atlantic continental platform sediments. J. Mar. Res. 54, 1179–1205. https://doi.org/10.1357/0022240963213745.

Soetaert, K., Herman, P.M.J., 1995a. Nitrogen dynamics in the Westerschelde estuary (SW Netherlands) estimated by means of the ecosystem model MOSES. Hydrobiologia 311, 225–246. https://doi.org/10.1007/BF00008583.

Soetaert, K., Herman, P.M.J., 1995b. Carbon flows in the Westerschelde estuary (The Netherlands) evaluated by means of an ecosystem model (MOSES). Hydrobiologia 311, 247–266. https://doi.org/10.1007/BF00008584.

Soetaert, K., Herman, P.M.J., Kromkamp, J., 1994a. Living in the twilight: estimating net phytoplankton growth in the Westerschelde estuary (The Netherlands) by means of an ecosystem model (MOSES). J. Plankton Res. 16, 1277–1301. https://doi.org/10.1093/plankt/16.10.1277.

Soetaert, K., Herman, P.M.J., Scholten, H., 1992. Moses: Model of the Scheldt Estuary: Ecosystem Model Development under SENECA.

Soetaert, K., Middelburg, J.J., Heip, C., Meire, P., van Damme, S., Maris, T., 2006. Long-term change in dissolved inorganic nutrients in the heterotrophic Scheldt estuary (Belgium, The Netherlands). In: Limnology and Oceanography. American Society of Limnology and Oceanography Inc., pp. 409–423. https://doi.org/10.4319/lo.2006.51.1_part_2.0409

Soetaert, K., Vincx, M., Wittoeck, J., Tulkens, M., van Gansbeke, D., 1994b. Spatial patterns of westerschelde meiobenthos. Estuar. Coast Shelf Sci. 39, 367–388. https://doi.org/10.1006/ecss.1994.1070.

Statham, P.J., 2012. Nutrients in estuaries — an overview and the potential impacts of climate change. Sci. Total Environ. 434, 213–227. https://doi.org/10.1016/j.scitotenv.2011.09.088.

Struyf, E., van Damme, S., Gribsholt, B., Meire, P., 2005a. Freshwater marshes as dissolved silica recyclers in an estuarine environment (Schelde estuary, Belgium). Hydrobiologia 540, 69–77. https://doi.org/10.1007/s10750-004-7104-0.

Struyf, E., van Damme, S., Gribsholt, B., Middelburg, J., Meire, P., 2005b. Biogenic silica in tidal freshwater marsh sediments and vegetation (Schelde estuary, Belgium). Mar. Ecol. Prog. Ser. 303, 51–60. https://doi.org/10.3354/meps303051.

Struyf, E., van Damme, S., Meire, P., 2004. Possible effects of climate change on estuarine nutrient fluxes: a case study in the highly nutrified Schelde estuary (Belgium, The Netherlands). Estuar. Coast Shelf Sci. 60, 649–661. https://doi.org/10.1016/j.ecss.2004.03.004.

Terai, H., Goto, N., Mitamura, O., 2000. Seasonal variation in primary production of microphytobenthos at the Isshiki intertidal flat in Mikawa Bay. Limnology 1, 133–138. https://doi.org/10.1007/s102010070019.

Thouzeau, G., Grall, J., Clavier, J., Chauvaud, L., Jean, F., Leynaert, A., ni Longphuirt, S., Amice, E., Amouroux, D., 2007. Spatial and temporal variability of benthic biogeochemical fluxes associated with macrophytic and macrofaunal distributions in the Thau lagoon (France). Estuar. Coast Shelf Sci. 72, 432–446. https://doi.org/10.1016/j.ecss.2006.11.028.

Underwood, G.J.C., Kromkamp, J., 1999. Primary production by phytoplankton and microphytobenthos in estuaries. Adv. Ecol. Res. 29, 93–153. https://doi.org/10.1016/S0065-2504(08)60192-0.

van Colen, C., Rossi, F., Montserrat, F., Andersson, M.G.I., Gribsholt, B., Herman, P.M.J., Degraer, S., Vincx, M., Ysebaert, T., Middelburg, J.J., 2012. Organism-sediment interactions govern post-hypoxia recovery of ecosystem functioning. PLoS One 7, e49795. https://doi.org/10.1371/journal.pone.0049795.

van Damme, S., Struyf, E., Maris, T., Ysebaert, T., Dehairs, F., Tackx, M., Heip, C., Meire, P., 2005. Spatial and temporal patterns of water quality along the estuarine salinity gradient of the Scheldt estuary (Belgium and The Netherlands): results of an integrated monitoring approach. Hydrobiologia 540, 29–45. https://doi.org/10.1007/s10750-004-7102-2.

van den Meersche, K., Soetaert, K., Middelburg, J.J., 2011. Plankton dynamics in an estuarine plume: a mesocosm 13C and 15N tracer study. Mar. Ecol. Prog. Ser. 429, 29–43. https://doi.org/10.3354/meps09097.

van den Meersche, K., van Rijswijk, P., Soetaert, K., Middelburg, J.J., 2009. Autochthonous and allochthonous contributions to mesozooplankton diet in a tidal river and estuary: integrating carbon isotope and fatty acid constraints. Limnol. Oceanogr. 54, 62–74. https://doi.org/10.4319/lo.2009.54.1.0062.

Vanderborght, J.-P., Folmer, I.M., Aguilera, D.R., Uhrenholdt, T., Regnier, P., 2007. Reactive-transport modelling of C, N, and O2 in a river–estuarine–coastal zone system: application to the Scheldt estuary. Mar. Chem. 106, 92–110. https://doi.org/10.1016/j.marchem.2006.06.006.

Wang, Z.B., Vandenbruwaene, W., Taal, M., Winterwerp, H., 2019. Amplification and deformation of tidal wave in the upper Scheldt estuary. Ocean Dynam. 69, 829–839. https://doi.org/10.1007/s10236-019-01281-3.

Wollast, R., Peters, J.J., 1978. Biogeochemical properties of an estuarine system: the River Scheldt. In: Goldberg, E.D. (Ed.), Biogeochemistry of Estuarine Sediments. UNESCO, Paris, pp. 279–293.

Zapata, M., Rodríguez, F., Garrido, J., 2000. Separation of chlorophylls and carotenoids from marine phytoplankton:a new HPLC method using a reversed phase C8 column and pyridine-containing mobile phases. Mar. Ecol. Prog. Ser. 195, 29–45. https://doi.org/10.3354/meps195029.

Zhang, J.Z., Huang, X.L., 2011. Effect of temperature and salinity on phosphate sorption on marine sediments. Environ. Sci. Technol. 45, 6831–6837. https://doi.org/10.1021/es200867p.